Ocean Engineering 79 (2014) 10–25

Contents lists available at ScienceDirect

Ocean Engineering

journal homepage: www.elsevier.com/locate/oceaneng

An algorithm for offline identification of ship manoeuvring mathematical models from free-running tests

Serge Sutulo, C. Guedes Soares *

Centre for Marine Technology and Engineering (CENTEC), Instituto Superior Técnico, University of Lisbon, Av. Rovisco Pais, 1049-001 Lisbon, Portugal

ARTICLE INFO

Article history:
Received 25 May 2013
Accepted 8 January 2014
Available online 30 January 2014

Keywords:
Ship manoeuvrability
Mathematical model
System identification
Genetic algorithm
White noise
Hausdorff's metric

ABSTRACT

An identification algorithm for ship manoeuvring mathematical models has been developed. The identification procedure is based on the classic genetic algorithm used for minimizing a distance between the reference and recovered time histories. The distance was measured using 5 different metrics including the Hausdorff metric. Validation of the algorithm was carried out using simulated responses artificially polluted with the white noise of various levels. It was demonstrated that by only using the Hausdorff metric it was possible to reach necessary robustness of the identification algorithm.

1. Introduction

Capability to create highly accurate mathematical models for adequate simulation of the manoeuvring motion of real vessels is of great practical value, primarily due to the ever increasing demand by numerous ship handling simulation centres, as well as by enterprises developing computer-based bridge simulators. In the ideal case, the simulated motion must be undistinguishable from the real one as the training process will be then the most effective. Of course the full realism is never reachable but it can and must be approximated as closely as possible. The realism and adequacy of the manoeuvring simulation depends on several factors which include: (1) accurate reproduction of the visual and—to a lesser extent—of the acoustic environment; (2) reproduction of tilts and accelerations possibly felt by the operator during manoeuvring; and (3) identity of responses of the original physical object and of its numerical models to the control actions.

Quality of visualization has increased very strongly during last 30 years resulting in 360° simulators, high-resolution screens and 3D visualization. Although the generated picture is and will remain for long much inferior in resolution to the real one, apparently this already does not represent a major problem that would significantly impair the simulation quality.

The tactile factors rarely are of substantial importance in marine simulations contrary to aeronautical applications but their modelling are desirable for high-speed craft, submarines and underwater vehicles. As there are no means for artificial generation of the gravitational field, the moving floor technique is used for both simulating actual tilts and centrifugal accelerations while the image is adjusted accordingly.

Adequacy of the core manoeuvring mathematical also can only be reached approximately: even the validation itself may present problems especially when it goes about the full model including effects of the hydrodynamic interactions, response to gusty wind and sea waves (Hensen, 1999). When talking about more standard situations, results of simulations can be, in principle, validated against full-scale measurements. But this still does not make simple the task of creation of an adequate mathematical model even when the full-scale data are accurate and reliable (which is rarely the case!). This is fundamentally caused by the fact that hydrodynamics of manoeuvring motion is of ultimate complexity representing a fusion and heavy generalization of the ship resistance, propulsion and seakeeping. All practical manoeuvring mathematical models are highly schematised and although in principle can be tuned to provide a satisfactory reproduction of the true motion, there are no simple theoretical methods for estimating their parameters. An attentive unbiased analysis of the problem soon reveals that the viscosity plays the major role in the formation of hydrodynamic forces related to manoeuvring and presence of strong separation phenomena makes the classic boundary layer theory absolutely insufficient while it used to be rather helpful in ship resistance. Hence, only models based on the full Naviers–Stokes equations can promise reliable prediction of manoeuvring forces.

In spite of great progress in computational fluid dynamics (CFD) and its successful applications to manoeuvrability (Stern

* Corresponding author. Tel.: +351 218417607; fax: +351 218474015.
E-mail address: c.guedes.soares@tecnico.ulisboa.pt (C. Guedes Soares).

0029-8018/$ - see front matter © 2014 Elsevier Ltd. All rights reserved.
http://dx.doi.org/10.1016/j.oceaneng.2014.01.007

et al., 2011) practical simulation-oriented mathematical models still are often devised on the basis of experimental data.

Due to various reasons, most modern ship mathematical models can be called "physical" or—to be more precise—"mechanical" as they are based on principles and equations of classic mechanics. Alternative approaches have created purely "input–output" models on the basis of artificial neural networks (ANN) (Faller et al., 1998; Moreira and Guedes Soares, 2003, 2012). The ANN algorithms may have certain advantages as they do not imply any *a priori* structure of the ship mathematical model. But the absence of any physical ground behind the ANN model represents, at the same time, a natural disadvantage of ANN models as they cannot be extended, modified or tuned without full retraining which is not always possible. The latter deficiency is to a large extent neutralized in the hybrid approach where a mechanical model is combined with ANN technique applied, replacing usual regressions, for representation of hydrodynamic forces (Rajesh and Bhattacharyya, 2008; Rajesh et al., 2010). Recently several studies have appeared on application of such a parental and presumably robust method as that of Support Vector Regressions/Machines (Luo and Zou, 2009; Zhang and Zou, 2011) but the validation carried out so far does not permit to draw definite conclusions about the effectiveness of this approach.

Any mathematical model based on mechanics implies presence of certain forces acting upon the ship and its elements depending on the parameters of motion. Most of these forces can be relatively easily measured on scaled models and their elements during the so-called captive-model tests. Results of these measurements can be used for construction of desired simulation models although these can be distorted by the scale effect (Sutulo and Guedes Soares, 2011). Unfortunately, most of the forces cannot be measured in full scale and while measuring, for instance, the propeller and rudder forces is in principle possible, it is very complicated and costly. At the same time, it is relatively simple to measure kinematical parameters during the motion resulting from some well-defined steering programme. In some sense, such full-scale tests or even tests with scaled free-running models (Moreira and Guedes Soares, 2011; Perera et al., 2012; Obreja et al., 2010; Araki et al., 2012) can be even easier to realize than to perform captive-model tests as no special facilities are required and full-scale data are typically necessary anyway for validation of implemented manoeuvring models. But if nothing more than kinematical measurements are available, the core manoeuvring mathematical model can only be reconstructed indirectly, via an identification procedure. Relatively rarely captive-model tests are combined with the free-running ones. For instance, Skjetne et al. (2004) have determined all forces not dependent on the yaw velocity from oblique captive tests carried out in a normal towing tank while the remaining part of the model was obtained from free-running model tests with online system identification.

If the structure of the mathematical model is established *a priori*, just the values of the parameters of the model are to be estimated and it goes then about the *parametric identification* and most of the applied studies belong to that group.

Primarily the identification problem was formulated and studied in the general system theory aiming at control applications (Ljung, 1987) as sufficient knowledge on the mathematical models of controlled or stabilised objects was necessary for synthesis of optimized and adaptive control laws let alone the importance of the simulation of control processes before final implementation of the synthesized controllers in real objects and systems.

Apparently, for the first time the identification problem with application to ship dynamics problems was formulated by Nomoto et al. (1957) who tried to make the problem treatable by very simple algorithms not requiring computer technology. It was assumed that the model is linear and it was further simplified having finally developed the famous Nomoto equations containing the minimum number of parameters which indeed could be easily estimated after a zigzag test. Although the Nomoto equations proved to be useful in certain applications, like synthesis of controllers and short-term predictions, their linearity and the reduced number of parameters made them unsuitable for realistic simulations. As to the simplest first-order Nomoto equation, it was even demonstrated (Sutulo and Guedes Soares, 2004) that it possesses no non-trivial parameters at all!

That is why, most of the manoeuvring model parameters identification studies were based on more complicated multi-parameter models. Elementary identification is then impossible. Often the models are tuned manually before being implemented in bridge simulators although such approaches are rarely even mentioned in the literature. In these cases, it is possible to talk, in fact, about a kind of interactive manual identification process which is, however, slow, tedious and depending on human skills.

Hence, sophisticated numerical methods were applied, part of them custom-devised but mostly used as they had been developed in the control theory (Ljung, 1978; Garnier and Wang, 2008).

All identification algorithms can be divided into two main groups: *online* procedures and *offline* procedures. According to Ljung and Söderström (1983) "the offline identification is the determination of a model of a system using a batch of measured data where the whole batch is available at all stages of the procedure". This is exactly the situation faced in all experimental studies when the identification becomes part of the post-processing. On the contrary, the online identification presumes the measuring and identification processes running in parallel though typically with a certain lag of the latter. As long as additional data are fed into the identification procedure the quality of the estimated model is constantly improved and/or modified together with the modification of the "true" model. This quality is valuable for applications to optimized and adaptive controllers although in general a suitable offline procedure will be always superior in the situations when the both approaches can be applied.

In spite of this more or less evident consideration, first applications of the system identification to ship dynamics were based on such a classic online method as the Extended Kalman Filter (EKF) (Brinati and Rios Neto, 1975; Åström and Källström, 1976; Källström and Åström, 1981; Abkowitz 1980, 1988). Although this method typically demonstrated slow convergence requiring long records, the EKF or similar recursive estimators like Unscented Kalman Filter, Modified Bryson–Frazier fixed interval smoother and others kept unparalleled popularity (Zhou and Blanke, 1987; Rhee and Kim, 1999; Yoon and Rhee, 2003; Araki et al., 2012; Revestido Herrero and Velasco González, 2012). A characteristic feature of the latter study is that the parametric identification was combined with the significance analysis applied to a rather simple quasi-polynomial model for hydrodynamic forces. In most cases, however, this analysis is performed in advance using available captive-model test results and applying physical considerations.

The adaptive backstepping method was applied by Casado et al. (2007) to only a highly simplified and easy to identify ship mathematical model (1st order Nomoto equation with a simple nonlinearity added), so, in fact, nothing can be said about its real effectiveness.

It was discovered very soon that the problem of identifying parameters of a rather complex and realistic ship manoeuvring model is ill-posed and at high noise levels typical for the sea trials data heavily biased estimates and, as result, useless models could be obtained. Abkowitz (1980, 1988) was only able to fight the observed cancellation effect through elimination of "inconvenient" terms which, however, could lead to models with limited applicability as certain regression terms may only become significant in special conditions like sailing in wind.

The problem of ill-posedness can be easier treated in offline algorithms which are allowed to be slower and more

complicated. Silman (1988) proposed two relatively efficient deterministic offline methods. The first method combined minimization of the Euclidean metric of the fitting error by the Gauss–Newton method combined with the functional regularization and multi-criterial optimization. The regularization was necessary because the objective function turned out multimodal and a local optimization method could easily converge to a "wrong" extremum. The second method overrode this problem by being based on the quasi-random global search in the parameter space with a number of *a priori* constraints. Both methods were used successfully for practical identification but the identification process was in fact interactive and required tries and decisions from the user.

The offline identification method proposed by Di Mascio et al. (2011) was based on the genetic algorithm (GA). The used merit functions were here somewhat unusual as they were constructed as sums of discrepancies of such characteristic numerical measures as the advance, transfer and tactical diameter in turning, the zigzag overshoot angles etc. instead of typically used functionals of the response error. Comparison with a method based on a modified EKF showed clear inferiority of the latter but the proposed GA-based method still suffered from the mentioned cancellation effects.

Also, the so-called two-step method belonging to the offline family was implemented and tested in several variations. The idea of this method is to obtain time histories for the total quasi-steady hydrodynamic forces from the equations of ship dynamics viewed as the responses and records for the rudder angle, velocities and propeller rpm regarded as the input. The second step typically presumes performing regression analysis over the sets of inputs and responses although these could also be used to create grid functions which could be further used directly with the help of some interpolation procedure. Artyszuk (2007) tested this approach for a 4-quadrant ship mathematical model using artificial simulated records. This was the only one known attempt to identify a 4-quadrant model suitable for arbitrary manoeuvres but as the records did not contain any noise, the validation remained somewhat incomplete.

Yoon and Rhee (2003) used alternatively the EKF and the Modified Bryson–Frazier Smoother (MBFS) to filter the measured kinematical variable and to restore the time histories for the hydrodynamic forces and for the sway velocity which was not measured. The MBFS was shown to give substantially better results. At the second step, parameters of the polynomial regression model were estimated by means of the ridge regression and followed by analysis of multi-collinearity. It was concluded that the combination of a 20°–20° zigzag with the 35° turn was not rich enough to guarantee reliable estimation of all regression coefficients and optimized pseudo-random binary sequences were suggested as alternative.

Of substantial interest is the study (Araki et al., 2012) where three kinds of training time histories in 4DOF were processed: (1) after a database method which was used for primary validation of identification algorithms, (2) after simulation with a CFD code in the loop, and (3) after free-running model measurements. Identification was performed either using a more or less standard EKF technique applied to parameters of a modular (not completely polynomial) manoeuvring model or considering the modular model as a nonlinear regression structure whose parameters were estimated from force time histories using a constrained gradient minimization algorithm. However, a conclusion was drawn that only the EKF is suitable in all the cases including data from free-running models while the time histories for all force components were only judged available in CFD simulations.

Other reviews of studies on application of the system identification to ship manoeuvrability, more complete and elaborated in some respects, can be found in Sutulo and Guedes Soares (2011) and Revestido Herrero and Velasco González (2012).

In the present study, a new offline identification algorithm has been developed and tested on artificial data including ones heavily polluted with simulated white noise. The method is based on a GA driver minimizing some metric of the difference between the reference response and the response obtained with the identified parameters. The present implementation was made for a moderately complex 3DOF polynomial manoeuvring model and several metrics were tested. The standard zigzag manoeuvre was used for identification purposes but the identified model was further validated with the turning and spiral manoeuvres. Besides the development of the algorithm and the implementing code per se, the immediate goal of the present study was demonstration of the consistency of the method and selection of the best metric.

2. Ship mathematical model

Although the proposed identification algorithm is applicable to a manoeuvring mathematical model of arbitrary structure, in the present study it is applied to a 3DOF model mainly based on 3rd-order polynomial regressions for forces on the system hull–rudder augmented with a simple model for the propeller thrust and a first-order nonlinear model for the steering gear. The third-order polynomial regression model proved to be sufficient for adequate representation of hydrodynamic forces on a ship executing moderate manoeuvres (Viallon et al., 2012). In general, the model used here is of moderate complexity. On one hand, it is sufficiently simple and transparent for analysis and, on the other hand, identification of its parameters is definitely a non-trivial task.

2.1. Frames of reference and kinematic equations

The Earth-fixed axes $O\xi\eta$ lie on the undisturbed water surface, the direction of the ξ-axis corresponds to the approach course of the ship and the η-axis is obtained after rotation of the first axis clockwise by $\pi/2$. The body axes Cxy also lie on the undisturbed free surface, its origin C belongs to the intersection of the centerplane, with the midship plane, the x-axis is directed to the bow and the y-axis—to the starboard. The instantaneous position of the ship at a given time t is described by the coordinates of the origin: the advance $\xi_C(t)$ and transfer $\eta_C(t)$, and the heading (yaw) angle $\psi(t)$ positive clockwise.

The instantaneous motion of the ship is described by the instantaneous velocity $V(t)$ having the velocities of surge $u(t)$ and sway $v(t)$ as projections onto the body axes and by the rate of yaw $r(t)$.

Then the kinematic differential equations for the generalized coordinates will be:

$$\begin{aligned} \dot{\xi}_C &= u\cos\psi - v\sin\psi, \\ \dot{\eta}_C &= u\sin\psi + v\cos\psi, \\ \dot{\psi} &= r. \end{aligned} \tag{1}$$

2.2. Dynamic equations

The standard Euler equations for a ship considered as a rigid body moving in the horizontal plane are:

$$\begin{aligned} &(m+\mu_{11})\dot{u} - mvr - mx_G r^2 = X_q + X_P, \\ &(m+\mu_{22})\dot{v} + (mx_G+\mu_{26})\dot{r} + mur = Y_q, \\ &(mx_G+\mu_{26})\dot{v} + (I_{zz}+\mu_{66})\dot{r} + mx_G ur = N_q, \end{aligned} \tag{2}$$

where m is the mass of the ship, $\mu_{11},\ldots,\mu_{66}$ are the added mass coefficients, x_G is the abscissa of the centre of mass, I_{zz} is the moment of inertia in yaw, X_q, Y_q, N_q are the quasi-steady forces/moment on the hull and rudder in surge, sway, and yaw respectively, X_P is the surge force caused by the propeller (effective thrust).

The quasi-steady forces (including the yaw moment) depend on the actual rudder deflection angle δ_R which, however, is not necessarily identical to the desired (ordered) angle δ^*. Although in the purpose of the present study it could have been assumed $\delta_R \equiv \delta^*$ meaning an ideal steering gear, the necessity for accounting for the rudder angle saturation $|\delta_R| \le \delta_m$ and the rudder rate saturation $|\dot{\delta}_R| \le \varepsilon_m$ makes it more convenient to use the first-order nonlinear steering gear model

$$\dot{\delta}_R = F_R(\delta_R, \delta^*), \tag{3}$$

where the rather complicated explicit description of the nonlinear function $F_R()$ is given in the authors' article (Sutulo and Guedes Soares, 2014).

2.3. Parameters of the manoeuvring model

The ship manoeuvring mathematical model in its hydrodynamic respect was constructed combining the model for the hull surge forces as proposed by Inoue et al. (1981) with the polynomial regressions obtained by Strom-Tejsen for the *Mariner* class ship as presented by Crane et al. (1989). While the base values of most parameters are mainly valid for just the *Mariner* ship, the model was augmented through introduction of a coefficient simulating alterations in the rudder area and by correcting some coefficients for the trim using formulae proposed by Inoue et al. (1981). The trim is not necessarily actual: a fictitious trim can be introduced just to vary manoeuvring qualities of a ship. The model was brought to a unified form required by the in-house offline manoeuvring simulation programme developed by the authors (Sutulo and Guedes Soares, 2005a). It must be noticed, however, that the resulting model should not be regarded as that of a Mariner type ship but rather of some realistic generic vessel.

The forces at the right-hand side of Eq. (3) are represented as

$$X_q = X'_q\frac{\rho V^2}{2}LT, \quad Y_q = Y'_q\frac{\rho V^2}{2}LT, \quad N_q = N'_q\frac{\rho V^2}{2}L^2T, \tag{4}$$

where X', Y', and N' are the dimensionless force/moment coefficients, ρ is the water density, $V^2 = u^2 + v^2$ is the squared instantaneous ship speed, L is the length of the ship and T is its draught at the midship.

The dimensionless forces are defined as multi-variate third-order regression polynomials depending, besides of the rudder angle, on the non-dimensional velocities $u' = u/V$, $v' = v/V$; $r' = rL/V$:

$$\begin{aligned}
X'_q &= X'_{uu}u'^2 + X'_{vr}v'r' + X'_{\delta\delta}\delta_R^2,\\
Y'_q &= Y'_0 + Y'_v v' + Y'_r r' + Y'_{vvv}v'^3 + Y'_{vvr}v'^2r' + Y'_\delta\delta_R + Y'_{vv\delta}v'^2\delta_R + Y'_{v\delta\delta}v'\delta_R^2,\\
N'_q &= N'_0 + N'_v v' + N'_r r' + N'_{vvv}v'^3 + N'_{vvr}v'^2r' + N'_\delta\delta_R + N'_{vv\delta}v'^2\delta_R + N'_{v\delta\delta}v'\delta_R^2 + N'_{\delta\delta\delta}\delta_R^3,
\end{aligned} \tag{5}$$

where $X'_{uu},\ldots,N'_{\delta\delta\delta}$ are the regression coefficients (also traditionally called "hydrodynamic derivatives") which are supposed to be defined and constant for a "true" mathematical model but they are adjustable through an identification process.

It can be noticed that the term $Y'_{\delta\delta\delta}\delta_R^3$ is absent as it was found less significant in the study carried out by Viallon et al. (2012) although this is not essential for the present study.

The coefficients in (5) are defined as:

$$\begin{aligned}
&X'_{uu} = -\kappa_{xuu}\tfrac{2mC_{TL}}{L^2T}; \quad X'_{vr} = -\kappa_{xvr}\tfrac{1.3\mu_{22}}{L^2T}; \quad X'_{\delta\delta} = k_R\kappa_{x\delta\delta}X'_{\delta\delta0};\\
&Y'_0 = \kappa_{y0}Y'_{00}; \quad N'_0 = \kappa_{n0}N'_{00}; \quad Y'_v = \kappa_{yv}(1+b_1\tau')Y'_{v0}; \quad Y'_r = \kappa_{yr}(1+b_2\tau')Y'_{r0};\\
&N'_v = \kappa_{nv}(1+b_3\tau')N'_{v0}; \quad N'_r = \kappa_{nr}(1+b_4\tau')(N'_{r0}+m'x'_Gu'); \quad Y'_\delta = k_R\kappa_{y\delta}Y'_{\delta0};\\
&N'_\delta = k_R\kappa_{n\delta}N'_{\delta0}; \quad Y'_{vvv} = \kappa_{yvvv}Y'_{vvv0}; \quad N'_{vvv} = \kappa_{nvvv}N'_{vvv0}; \quad Y'_{vvr} = \kappa_{yvvr}Y'_{vvr0};\\
&N'_{vvr} = \kappa_{nvvr}N'_{vvr0}; \quad Y'_{\delta vv} = k_R\kappa_{y\delta vv}Y'_{\delta vv0}; \quad N'_{\delta vv} = k_R\kappa_{n\delta vv}N'_{\delta vv0};\\
&Y'_{\delta\delta v} = k_R\kappa_{y\delta\delta v}Y'_{\delta\delta v0}; \quad N'_{\delta\delta v} = k_R\kappa_{n\delta\delta v}N'_{\delta\delta v0}; \quad N'_{\delta\delta v} = k_R\kappa_{n\delta\delta\delta}N'_{\delta\delta\delta0},
\end{aligned} \tag{6}$$

where $\kappa_{xuu},\ldots,\kappa_{n\delta\delta\delta}$ are the adjustment coefficients; C_{TL} is the ship drag coefficient non-dimensionalised by $(m/L)V^2$ (Van Maanen and Van Oossanen, 1988); k_R is the rudder area coefficient; $\tau' = (T_{\mathrm{STERN}} - T_{\mathrm{BOW}})/T$ is the relative trim; b_1, b_2, b_3, b_4 are constant coefficients; $m' = 2m/(\rho L^2 T)$ is the non-dimensional ship mass coefficient; $x'_G = x_G/L$ is the non-dimensional abscissa of the centre of mass; $X'_{\delta\delta0},\ldots,N'_{\delta\delta\delta0}$ are the base values of hydrodynamic derivatives.

The constant base parameters in Eq. (6) are defined using data from the sources mentioned above:

$$\begin{aligned}
&C_{TL} = 0.07; \quad Y'_{00} = -0.0008; \quad Y'_{v0} = -0.244; \quad Y'_{r0} = 0.067; \quad N'_{00} = 0.00059;\\
&N'_{v0} = -0.0555; \quad N'_{r0} = -0.0349; \quad m' = 0.172; \quad Y'_{vvv0} = -1.702; \quad N'_{vvv0} = 0.345;\\
&Y'_{vvr0} = 3.23; \quad N'_{vvr0} = -1.158; \quad Y'_{\delta0} = -0.0586; \quad N'_{\delta0} = 0.0293; \quad X'_{\delta\delta0} = -0.02;\\
&Y'_{\delta vv0} = -0.25; \quad N'_{\delta vv0} = -0.1032; \quad Y'_{\delta\delta v0} = -0.0008; \quad N'_{\delta\delta v0} = 0.00264;\\
&N'_{\delta\delta\delta0} = -0.00482; \quad b_1 = 0.6667; \quad b_2 = 0.8; \quad b_3 = -0.27Y'_{v0}/N'_{v0}; \quad b_4 = 0.3.
\end{aligned} \tag{7}$$

The propeller force was described by the 4-quadrant model proposed by Oltmann and Sharma (1985) for a specific propeller but adjusted to the hull hydrodynamics by means of the adjustment procedure described in Sutulo and Guedes Soares (2011). The propeller surge force X_P is the same as the effective thrust $T_E = (1-t_P)\frac{\rho}{2}A_dC_TV_B^2$, where t_P is the thrust deduction coefficient, A_d is the propeller disk area, and

$$\begin{aligned}
&C_T = \begin{cases} C_{T0} + C_T^c c_B + C_T^s s_B & \text{at } c_B \ge 0.9336 \\ C_T^{cc}|c_B|c_B + C_T^{ss}|s_B|s_B & \text{otherwise,} \end{cases}\\
&V_B^2 = u_A^2 + v_{CP}^2; \quad u_A = u(1-w_P); \quad v_{CP} = 0.7\pi D_P n;\\
&c_B = v_{CP}/V_B; \quad s_B = u_A/V_B; \quad C_{T0} = -0.833;\\
&C_T^c = 1.02; \quad C_T^s = -0.332; \quad C_T^{cc} = 0.099; \quad C_T^{ss} = -0.671,
\end{aligned} \tag{8}$$

where w_P is the wake fraction coefficient, D_P is the propeller diameter, n is the propeller rotation frequency (rps).

2.4. Formalized matrix representation of the manoeuvring model

Consider the following arithmetic vectors represented as column matrices:

– the vector of velocities and of the actual rudder angle

$$\mathbf{x}_1 = (u, v, r, \delta_R)^T; \tag{9}$$

– the vector of generalized coordinates

$$\mathbf{x}_2 = (\xi_C, \eta_C, \psi)^T; \tag{10}$$

– the full state vector as concatenation of the previous two

$$\mathbf{x} = (\mathbf{x}_1^T, \mathbf{x}_2^T)^T; \tag{11}$$

– the observation vector

$$\mathbf{y} = \mathbf{C}\mathbf{x} + \boldsymbol{\varepsilon}, \tag{12}$$

where $\boldsymbol{\varepsilon}(t)$ is the noise vector, $\dim\mathbf{y} \le \dim\mathbf{x}$ and $\mathbf{C}$ is a constant observation matrix of appropriate dimensions which will be discussed and specified later;

– the control vector

$$\mathbf{u} = (\delta^*, n)^T; \tag{13}$$

– the vector of adjustment parameters

$$\boldsymbol{\kappa} = (\kappa_{xuu}, \kappa_{xvr}, \ldots, \kappa_{n\delta\delta\delta})^T, \tag{14}$$

which, however, does not necessarily include all adjustment coefficients shown in Eq. (6) and its dimension can vary.

Then, the mathematical model of the ship can be represented as

$$\dot{\mathbf{x}} = \mathbf{F}(\mathbf{x}, \mathbf{u}, \boldsymbol{\kappa}), \tag{15}$$

where $\mathbf{F}()$ is the column matrix function defined by the primary model description presented earlier.

The vector ordinary differential equation (15) must be complemented with the initial conditions vector $\mathbf{x}(0) = \mathbf{x}_0$. In the present study, all components of this vector will remain zero except for $u(0) = V_0$—the ship approach speed. In addition, the propeller rotation frequency was kept constant in all simulations performed in this study while the rudder order δ^* was considered a function of time or of the states depending on the manoeuvre simulated.

In the case of turning manoeuvres the control is purely feedforward i.e.

$$\delta^*(t) = \delta_T H(t), \tag{16}$$

where δ_T is the ordered constant helm and $H()$ is the Heavyside step function.

Other manoeuvres simulated in this study imply feedback control laws of the type $\delta^* = f(\mathbf{x})$. In the case of a zigzag manoeuvre the control law is rather simple:

$$\delta^*(r, \psi) = \delta_z \mathrm{sign}(\psi_z \mathrm{sign} r - \psi), \tag{17}$$

where δ_z and ψ_z are the common zigzag parameters.

The control law resulting in the Dieudonné spiral manoeuvre cannot be represented in a similarly compact form but its implementation presents no major problems anyway.

3. Identification problem formulation and method of solution

3.1. General remarks and metrics

It is supposed that there exist N reference training observed output processes $\{\mathbf{y}^{(i)}(t, \mathbf{u})\}_{i=1}^N$ where $t \in [0, T_0]$, T_0 is the duration of the process, and which can be viewed without loss of generality as only one compound reference process $\mathbf{y}(t, \mathbf{u})$. At any given adjustment vector $\boldsymbol{\kappa}$ the model defined by Eqs. (15) and (12) will produce at the same control $\mathbf{u}$ the response $\bar{\mathbf{y}}(t, \mathbf{u}, \boldsymbol{\kappa})$. Then the parametric (i.e. within the assumed model structure) identification consists in seeking such a value $\hat{\boldsymbol{\kappa}}$ of the adjustment vector $\boldsymbol{\kappa}$ which would minimize the distance between $\mathbf{y}(t, \mathbf{u})$ and $\bar{\mathbf{y}}(t, \mathbf{u}, \boldsymbol{\kappa})$ or, in other words:

$$\hat{\boldsymbol{\kappa}} = \underset{\boldsymbol{\kappa} \in \mathbf{K}}{\mathrm{argmin}} \rho(\mathbf{y}(t, \mathbf{u}), \bar{\mathbf{y}}(t, \mathbf{u}, \boldsymbol{\kappa})), \tag{18}$$

where $\mathbf{K}$ is the allowable domain for the adjustment vector, and $\rho()$ is some suitable metric.

The reference process $\mathbf{y}(t, \mathbf{u})$ is supposed to be obtained from full-scale trials or from tests with free-running models. In the present study, however, as no real suitable records were available, this process was generated using the mathematical model described above at $\boldsymbol{\kappa} = \mathbf{i}$, where $\mathbf{i}$ is the unity vector whose all components, i.e. the adjustment coefficients, are equal to 1.

Before some extremum search algorithm is applied to (18) the metric ρ must be defined. The distance between two vector responses $\mathbf{y} = (y_1, \ldots, y_n)^T$ and $\bar{\mathbf{y}} = (\bar{y}_1, \ldots, \bar{y}_n)^T$ of equal dimension n can be defined as

$$\rho(\mathbf{y}, \bar{\mathbf{y}}) = \sum_{i=1}^{n} \rho(y_i, \bar{y}_i), \tag{19}$$

where $\rho(y_i, \bar{y}_i)$ is a usual metric for scalar responses or values. It can be noticed that if ρ_0 is a metric, then $\varphi(\rho_0)$ is also a reasonably defined distance if $\varphi()$ is a strictly monotonous function i.e. such that $\varphi(x_1) > \varphi(x_2)$ if and only if $x_1 > x_2$ and $\varphi(0) = 0$. However, this derived distance or the *pseudo-metric* is not necessarily a true metric as the fulfilment of the triangle inequality, which is one of the metric axioms, cannot be guaranteed.

The following metrics were tried in the present study:

1. The Euclidean or L_2-metric

$$\rho_E(y, \bar{y}) = \left[\int_0^{T_0} (y(t) - \bar{y}(t))^2 dt\right]^{1/2}; \tag{20}$$

2. The square of the Euclidean metric

$$\rho_{E2}(y, \bar{y}) = \rho_E^2(y, \bar{y}); \tag{21}$$

3. The L_1-metric (also Abs-metric)

$$\rho_1(y, \bar{y}) = \int_0^{T_0} |y(t) - \bar{y}(t)| dt; \tag{22}$$

4. The C- or L_∞-metric (also L-infinity metric)

$$\rho_\infty(y, \bar{y}) = \max_{t \in [0, T_0]} |y(t) - y(\bar{t})|; \tag{23}$$

5. The Hausdorff metric (Rockafeller and Wets, 2004)

$$\rho_H(y, \bar{y}) = \max\{\sup_{t_1 \in [0,T_0]} \inf_{t_2 \in [0,T_0]} \rho_0(y(t_1), \bar{y}(t_2)), \sup_{t_2 \in [0,T_0]} \inf_{t_1 \in [0,T_0]} \rho_0(y(t_1), \bar{y}(t_2))\}, \tag{24}$$

where ρ_0 is some metric defined for real numbers, typically: $\rho_0(x, y) = |x - y|$.

3.2. Simulated manoeuvres

The choice of reference or training manoeuvres may be embarrassing as these must be relatively simple for execution including that in sea trials but, at the same time they must be sufficiently informative for reliable estimation of all parameters of interest. Ideally, the phase trajectories resulting from such manoeuvres should fill some sufficiently large domain in the state space but it is practically impossible to achieve with the standard means of control and some compromise must be assumed.

In the present study only the standard 20°–20° zigzag manoeuvre was used for training purposes in all the cases while the 35° turning manoeuvre and the Dieudonné spiral served for validation purpose only. Some impression about informative power of these manoeuvres can be obtained from the projections of the phase trajectories on the plane $\beta - r'$, where $\beta = -\arcsin v'$ is the drift angle. These projections are shown in Fig. 1, where, in addition, placed similar output for the weaker 10°–10° zigzag and for non-standard 30°–30° and 30°–60° zigzags although the phase portrait for the latter remained practically the same as for the former. It can be, first, concluded that the planned validation approach is not trivial as the validating manoeuvres provide different phase trajectories. It can be also anticipated that the 30°–30° zigzag would serve even better than the standard one but its investigation was not the aim of this paper. Also, the phase

trajectory projection generated by the PRBS rudder control is shown is in the same plot. The PRBS sampling time (Landau and Zito, 2006), i.e. the minimum time of constant helm, was 35 s and the helm amplitude was 30°. It is seen that the trajectory tends to fill the area bounded by the 30°–30° zigzag trajectory and thus the PRBS manoeuvre must be somewhat more informative. However, to achieve good loop filling, very long tests are required: for instance, the duration of the test presented in the plot was 3000 s in real time.

Rhee and Kim (1999) proposed and used the so-called S-type manoeuvre claiming that it was providing better information for the online EKF identification. However, this manoeuvre is nothing else than a biased zigzag and, for instance, the 60° (and more) S-manoeuvre with 30° rudder amplitude will have exactly the same phase portrait as the normal 30°–30°zigzag manoeuvre. The only difference somewhat affecting the identification results, as was reported by Rhee and Kim (1999), is the relative duration of the initial phase but the same effect could be achieved through application of appropriate weighting functions to the training data.

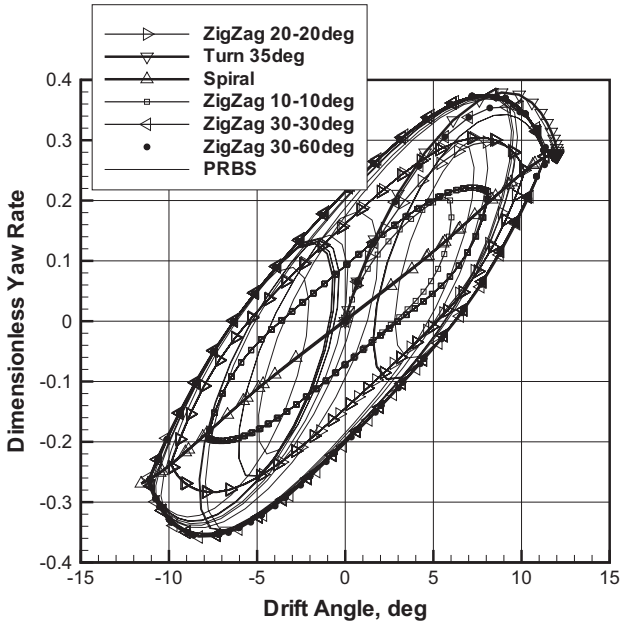

Fig. 1. Projections of phase trajectories for various manoeuvres (the phase portrait for the 30°–60° zigzag is almost undistinguishable from that of the 30°–30° zigzag).

Selection of observed responses constituting the vector **y** is not trivial. It could seem rather natural to use in this purpose the trajectory $(\xi_C(t),\ \eta_C(t))$ and the time history for the heading angle $\psi(t)$ and indeed so was done by many researchers. But these responses are very sensitive to the initial conditions of the velocities u, v, and r. It is clear from Eq. (1) that any uncertainties in the initial conditions of the velocities will result in unlimited growth of deviations from the true trajectory and from the true heading angle values. For instance, in the latter case the error grows linearly i.e. as $\delta\psi_0 t$, where $\delta\psi_0$ is the error in the initial condition for the heading. Due to inevitable presence of noise in the field records, it is usually difficult to estimate correctly the initial conditions.

Three possibilities can be considered to circumvent this problem:

1. Ignore the unknown initial conditions. But in this case one can expect obtaining biased estimates of the parameters of the model.
2. Include the unknown initial conditions into the vector of adjustable parameters. This is undesirable as increasing the dimension of the adjustment vector.

Table 1
Restored adjustment coefficients: case of "clean" records.

Subscript	Metric:				
	Euclidean	Euclidean Squared	Abs	L_∞	Hausdorff
22	1.01765	0.907843	1.08627	0.97451	0.915686
66	0.929412	1.09216	0.739216	1.08039	1.14118
xuu	0.990196	1.01765	1.01373	1.01765	1.01765
xδδ	0.909804	1.04902	0.998039	0.909804	0.74902
*y*0	0.852941	0.8	0.923529	1.09412	0.733333
yv	1.04314	0.939216	0.882353	0.84902	1.01961
yr	0.876471	0.752941	1.10588	1.17647	0.837255
yvvv	0.872549	0.794118	0.954902	0.884314	1.03725
yvvr	1.09804	0.786275	0.962745	0.839216	0.952941
yδ	1.04902	0.790196	0.94902	0.986275	0.886275
yδvv	0.847059	0.788235	0.927451	0.717647	1.0
*n*0	0.939216	1.01373	0.717647	1.02745	0.994118
nv	0.876471	0.927451	1.04314	0.980392	1.19216
nr	0.709804	1.17255	1.19216	1.14706	1.13137
nvvv	0.788235	0.95098	1.17059	0.762745	0.990196
nvvr	1.07843	1.04118	1.13529	1.04118	1.17451
nδ	0.9	1.09412	1.09804	1.08431	1.0
nδvv	1.13725	0.917647	1.17647	1.07451	1.11569
nδδδ	1.1451	1.09412	0.931373	0.913725	0.94902

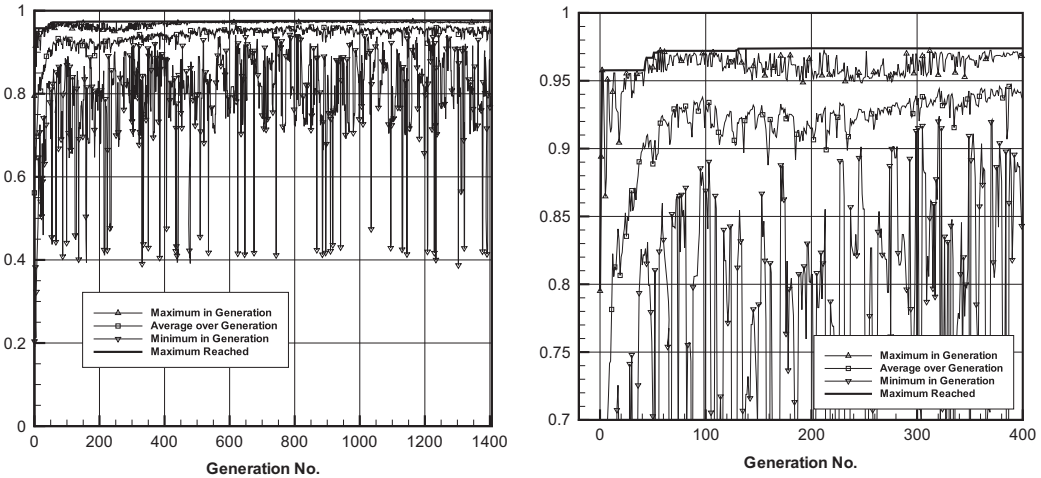

Fig. 2. Evolution of the fitness function values with the Hausdorff metric: right—zoomed initial part.

3. Exclude all generalized coordinates from the observation vector. This will result in the observation matrix $\mathbf{C} = \mathrm{diag}\,(1,1,1,1,0,0,0)$. Of course, this does not eliminate completely the influence of initial conditions but makes it weaker.

The third option was followed in the present study which means that two manoeuvring mathematical models are considered close to each other when during any manoeuvre close are time histories for the rudder angle, velocities of surge and sway and for the rate of yaw:

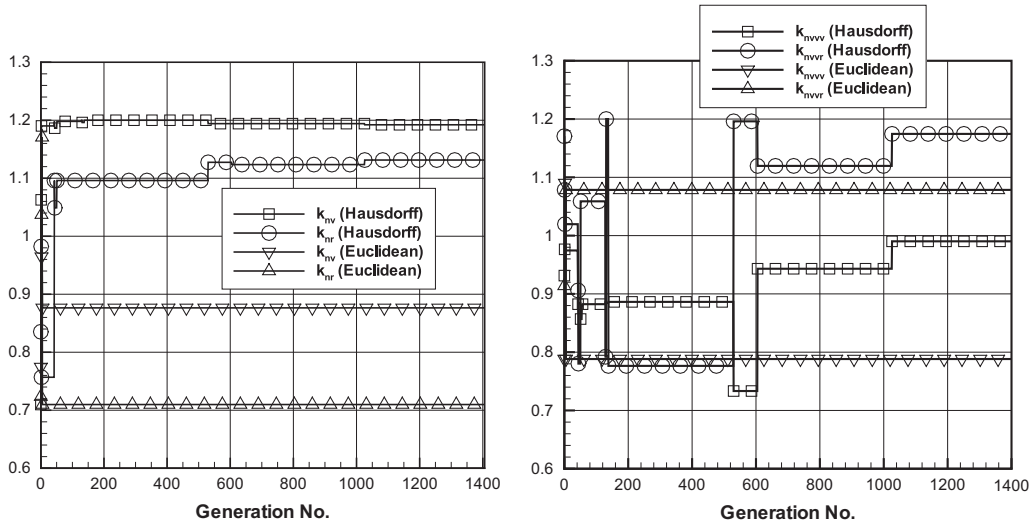

Fig. 3. Evolution of adjustment coefficients for Euclidean and Hausdorff metrics: left—linear terms; right—nonlinear terms.

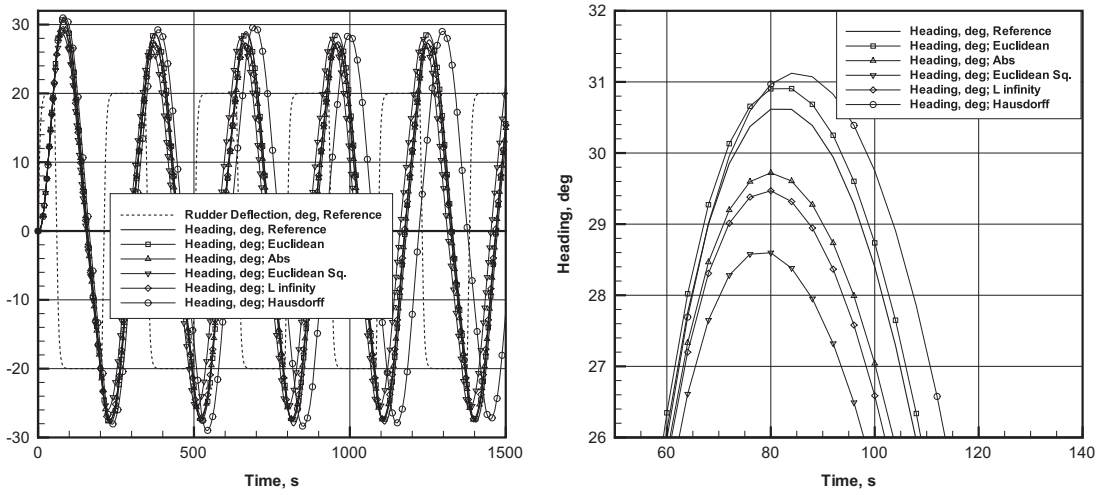

Fig. 4. Time histories in zigzag for reference and restored models: left—full, right—fragment.

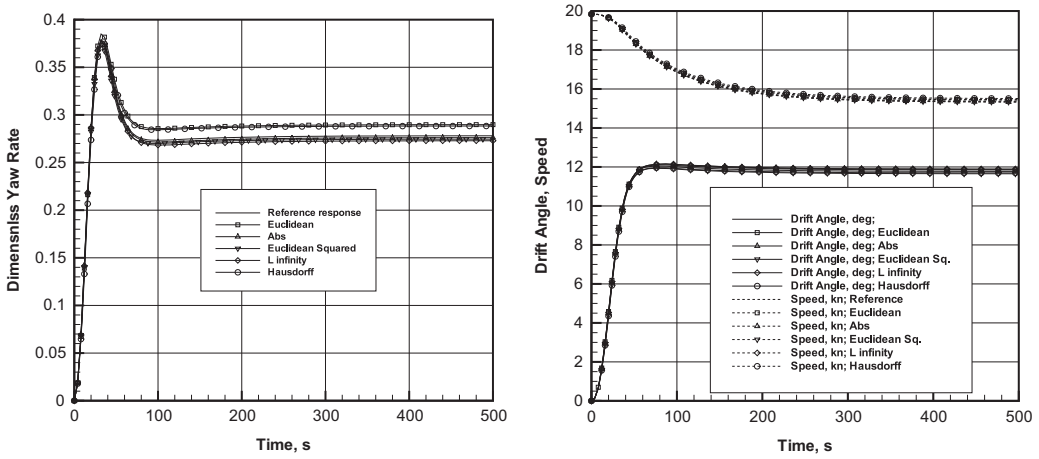

Fig. 5. Time histories for 35° turning manoeuvre for reference and restored models.

$\delta_R(t)$, $u(t)$, $v(t)$, $r(t)$. In fact this approach is very natural because in the practical ship steering no one expects from the vessel following some desired trajectory or even heading without feedback control because of presence of disturbances in real environment. In the introduced set of parameters assumed here to be observable the couple (u, v) is, obviously, equivalent to the couple (V, β). Nowadays, the drift angle can be certainly viewed as observable as in full-scale or free-running model trials can be calculated as the difference between the heading measured by the gyrocompass and the course-over-the-ground angle provided by the GPS receiver. In earlier studies carried out in the pre-GPS era the drift angle was often regarded as an unobservable estimated parameter which certainly aggravated the ill-posedness of the identification problem and practically made its good solution unlikely.

3.3. Optimization method

Eq. (18) presumes that some numerical optimization method must be used to find the estimated vector of adjustment coefficients $\hat{\boldsymbol{\kappa}}$. In this study an in-house optimizing driver based on the classical (binary) genetic algorithm (GA) was used. This algorithm was earlier used by the authors as part of synthesis of optimal experimental designs (Sutulo and Guedes Soares, 2005b) and in that application it demonstrated clear superiority over the quasi-random search.

This algorithm deals with haploid individuals represented as binary vectors of constant length conditioned by the dimension of the problem and by the required precision of coding which was chosen moderate in the present application: the length of a chromosome segment was 8 bits. Simple binary coding was used as well as the standard set of three main genetic operators: reproduction, the one-point crossover (with probability 0.6), and the single-bit mutation (with probability 0.001). The remainder stochastic sampling without replacement was used as the selection scheme and the σ-truncation combined with the linear scaling was used as objective function scaling procedure. The size of the population was 30 individuals. The optimization process was assumed to be converged if both the current best fitness and the best attained fitness were remaining the same during 200 generations in a row. However, the maximum allowed total number of generations was 2000.

4. Verification and validation of the identification algorithm

4.1. Case of "clean" simulated records

First, the zigzag manoeuvre was simulated at $\boldsymbol{\kappa} = \mathbf{i}$ with the 400 points output discretization at 1 Hz sampling frequency. After that, the identification procedure was run with the following options:

1. Some of the adjustment coefficients shown in (6) were fixed, namely it was assumed that $\kappa_{xvr} \equiv \kappa_{y\delta\delta v} \equiv \kappa_{n\delta\delta v} \equiv 1$. This decision was taken on the basis of the authors' previous numerical experiments and was aimed at reducing the dimension of the parameter space.
2. However, additional adjustment factors κ_{22} and κ_{66} were applied to the added mass coefficients μ_{22} and μ_{66}, so the vector $\boldsymbol{\kappa}$ had the size 19.
3. The initial value of the adjustment vector was obtained by assigning to each its component an independent random value in the interval [0.7, 1.3] which corresponds to typical uncertainties in estimating manoeuvring derivatives by theoretical or database methods. The same interval determined also the search domain for each component of the adjustment vector.

Then the GA was run with different metrics activated. An example of the evolution of the sum of distances between the reference and the restored responses is shown in Fig. 2 and the resulting values of the adjustment coefficients—in Table 1.

Although an "ideal" testing identification should have resulted in all values of the adjustment factors equal to 1, this did not actually happen. However, that is exactly what could be expected from a randomized global optimization algorithm with limited accuracy of data coding and, moreover, the recover of the "true" values of the parameters was not considered here as a goal of the identification process as in real life such "true" values do not exist at all (i.e. they are unobservable). On the other hand, in most cases deviation from the ideal value depending on the chosen metric does not exceed 20%. Some examples of the evolution of several adjustment coefficients are shown in Fig. 3. It can be noticed the GA "works" more actively when the Hausdorff metric is applied and with nonlinear coefficients. With the Euclidean metric final values of the considered coefficients were reached immediately.

The most important, however, is that the reference zigzag manoeuvre was restored with good precision (Fig. 4) which is even

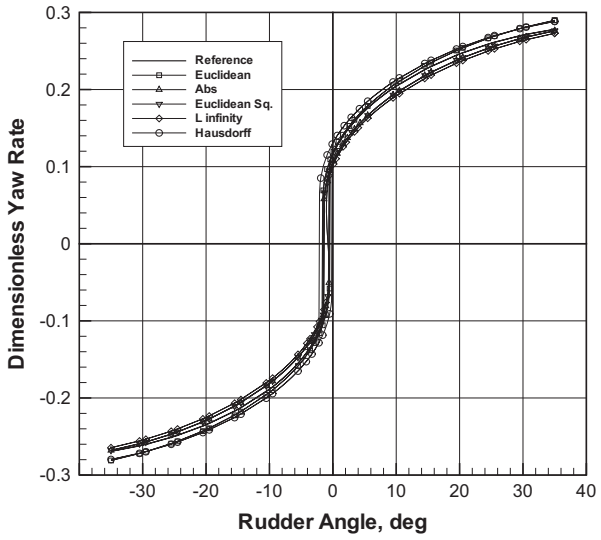

Fig. 6. Spiral curves for reference and restored models.

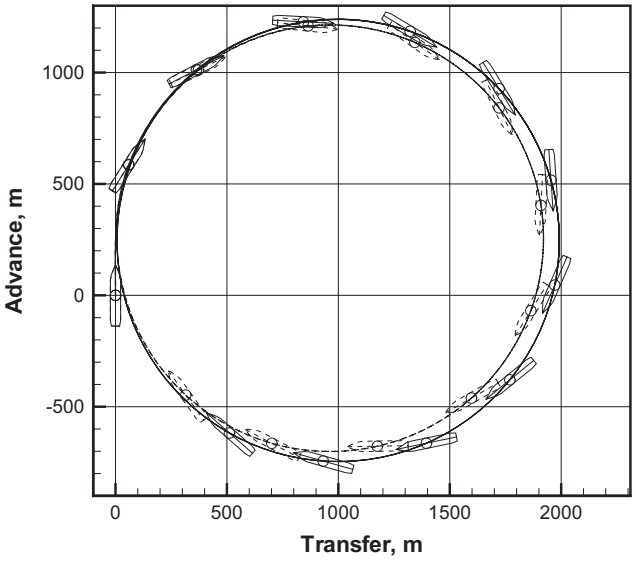

Fig. 7. Turning manoeuvre trajectories (identified from clean records): solid line—reference model; dashed line—Hausdorff metric.

more remarkable regarding that the yaw angle response was not used for identification. All metrics lead to approximately the same quality of results except for the Hausdorff metric which resulted in somewhat larger, although still acceptable, discrepancies.

Validation on the manoeuvres not used for identification also turned out successful: the time histories for the turning manoeuvre are shown in Fig. 5 and the reference and recovered spiral curves—in Fig. 6.

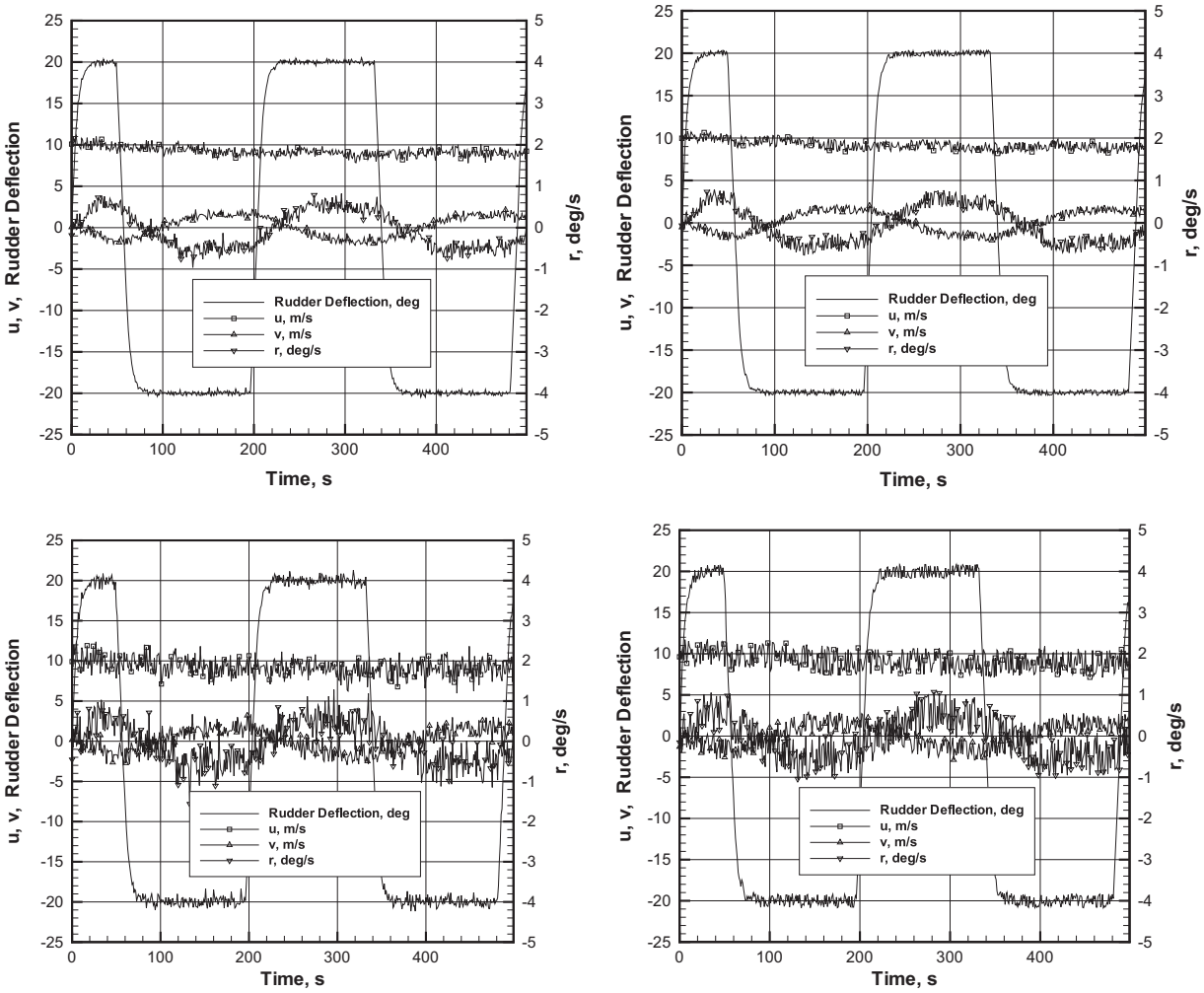

Fig. 8. Examples of artificially polluted responses in simulated manoeuvres: left—Gauss, right—uniform; top—20%, bottom—50%.

Table 2
Restored adjustment coefficients: case of records with 50% Gauss noise.

Subscript	Metric:				
	Euclidean	Euclidean Squared	Abs	L_∞	Hausdorff
22	0.854902	0.788235	0.854902	1.00196	0.711765
66	1.16078	0.943137	1.16078	1.05294	0.784314
xuu	1.19608	1.18431	1.19608	1.1902	1.19608
xδδ	1.15882	1.13725	1.15882	0.884314	1.13922
*y*0	0.827451	1.05294	0.827451	0.960784	0.711765
yv	0.75098	0.939216	0.75098	1.04902	1.08431
yr	0.801961	0.819608	0.801961	1.14706	1.19412
yvvv	0.94902	0.933333	0.94902	0.792157	1.10392
yvvr	0.9	0.709804	0.9	1.01569	0.833333
yδ	0.931373	1.08431	0.931373	0.866667	1.16863
yδvv	0.901961	0.882353	0.901961	0.988235	0.92549
*n*0	1.11765	0.921569	1.11765	0.882353	1.06667
nv	1.16471	1.19804	1.16471	1.00588	1.07255
nr	0.778431	0.701961	0.778431	1.17451	0.82549
nvvv	0.890196	1.02941	0.890196	0.992157	1.1098
nvvr	1.10392	1.13529	1.10392	1.11373	1.1451
nδ	0.707843	1.17647	0.707843	0.723529	0.786275
nδvv	1.19216	0.947059	1.19216	1.10588	0.756863
nδδδ	1.01569	0.903922	1.01569	0.82549	0.864706

As commented earlier, agreement of the ship trajectories is not considered in the present study as a very important criterion but, as traditionally it was viewed as such in numerous publications, trajectories for the 35° turning manoeuvre are presented in Fig. 7 for the Hausdorff metric only as trajectories obtained with the remaining metrics except the Euclidean metric were almost identical to reference trajectory while the Euclidean metric gave the same trajectory as the Hausdorff metric. However, it would be premature to conclude that

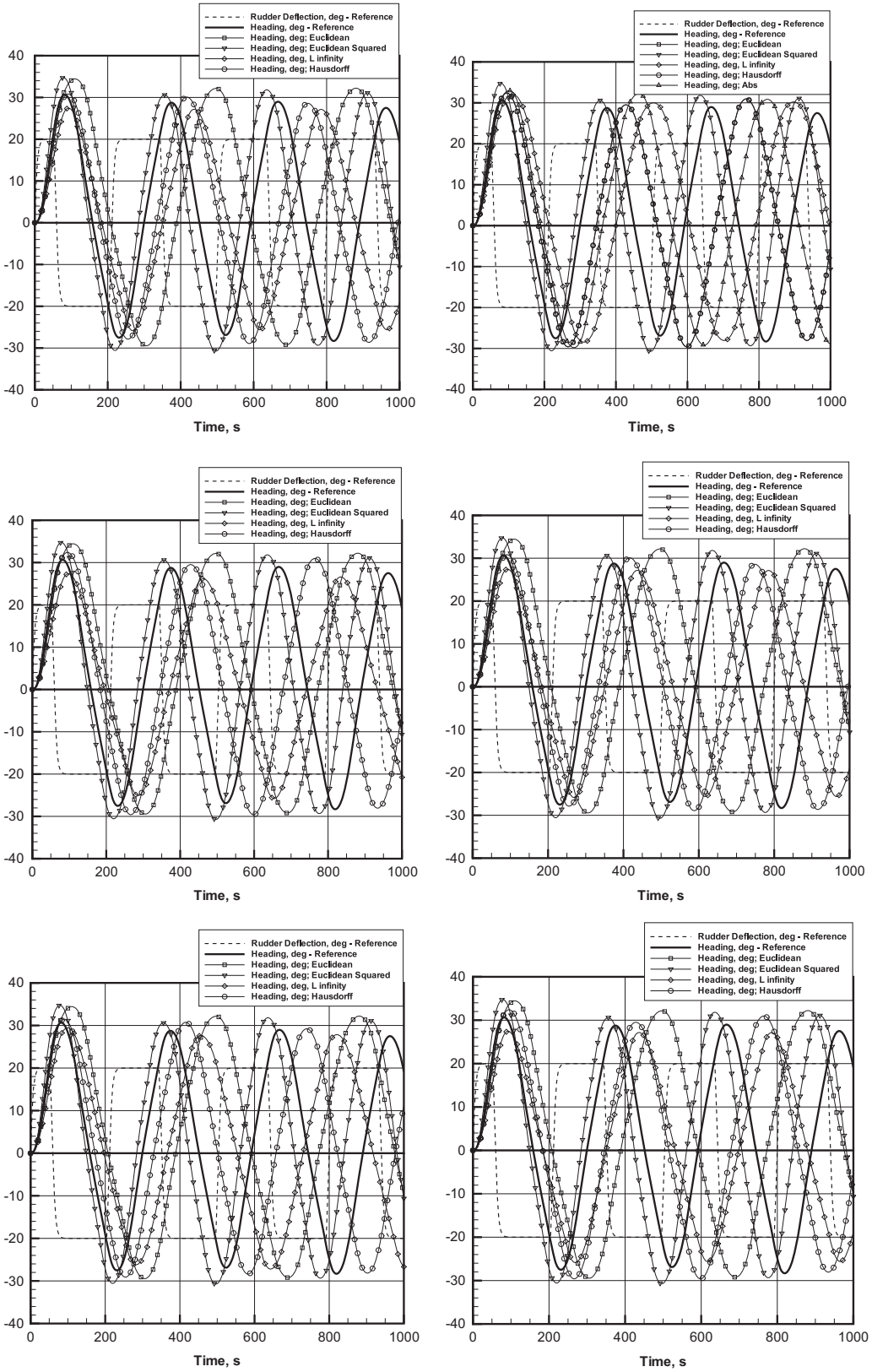

Fig. 9. Time histories in zigzag for reference and restored models: left—Gauss noise, right—uniform noise; top—noise 5%, middle—noise 20%, bottom—noise 50%.

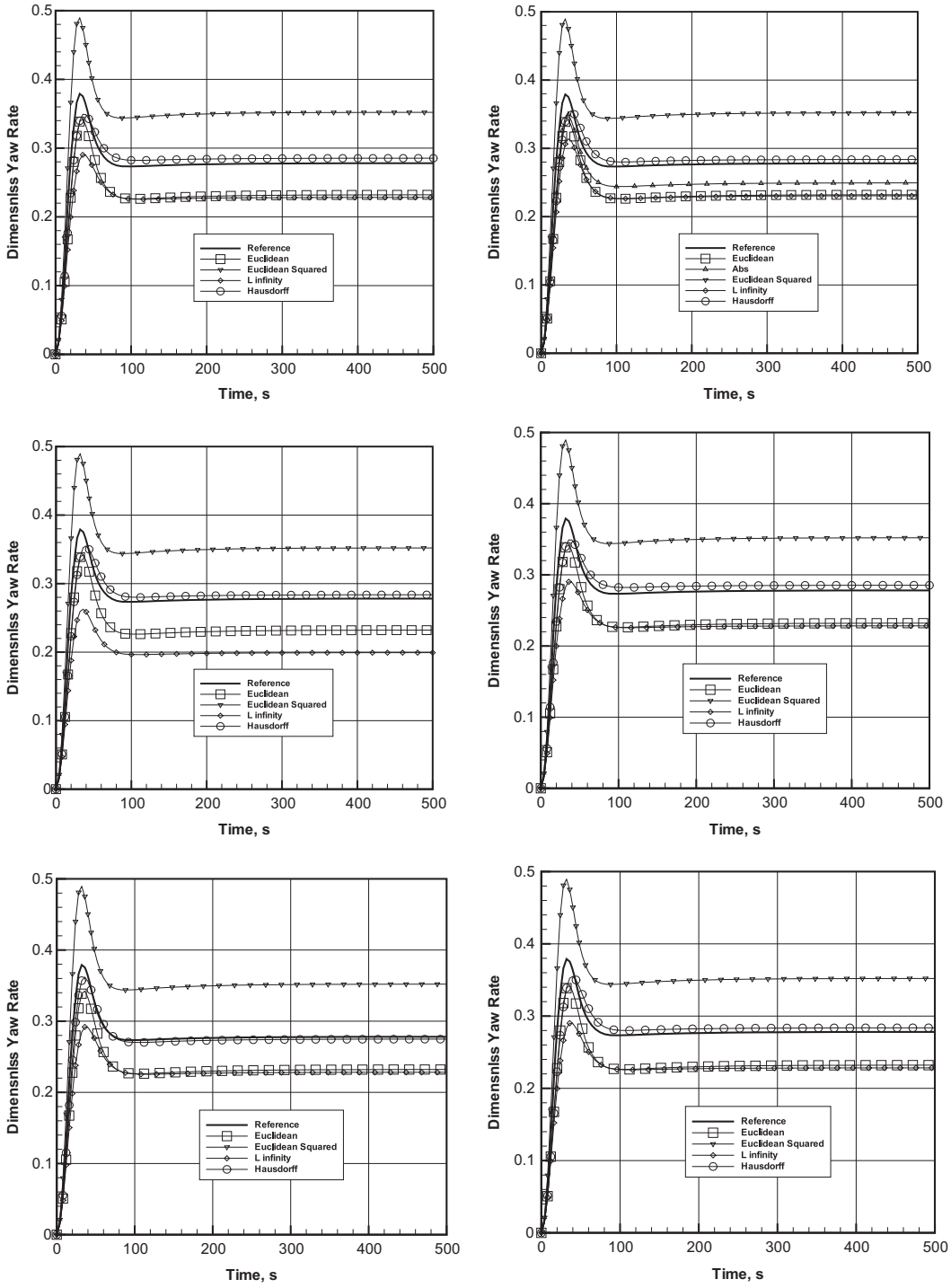

Fig. 10. Time histories $r'(t)$in the turning manoeuvre for reference and restored models: left—Gauss noise, right—uniform noise; top—noise 5%, middle—noise 20%, bottom—noise 50%.

these two metrics are inferior to others: first, agreement must be considered as excellent even in these "worse" cases and, second, much more important is performance of the identification algorithm in presence of noise than with clean simulated time series.

4.2. Validation on "polluted" responses

To test robustness of the identification algorithm, the simulated discrete records $\{\zeta_i\}_{i=1}^{400}$, where $\zeta=\delta_R$, u, v, r, were artificially "polluted" with the white noise in the following way:

$$\zeta_i=\zeta_{0i}+\zeta^{\max}k_0k_\zeta\xi_i, \tag{25}$$

where ζ_{0i} is the primary "clean" reference response, $\zeta^{\max}$ is the maximum reached absolute value of the clean response, k_0 is the general reduction factor assumed here to be 5%, 20%, or 50%, k_ζ is the response-specific reduction factor, and ξ_i is a discrete random variable which was either Gauss-distributed with the unit variance, or uniformly distributed within the interval $[-\sqrt{3},+\sqrt{3}]$ and also possessing a unit variance. Typically, records for the rudder angle and for the ship speed are substantially less noisy than those for the rate of yaw and drift angle. That is why the factor k_ζ was set to 0.05 for the rudder angle response and 0.2 for the velocity of surge while it is equal to 1.0 for the remaining responses. Examples of artificially polluted records are presented

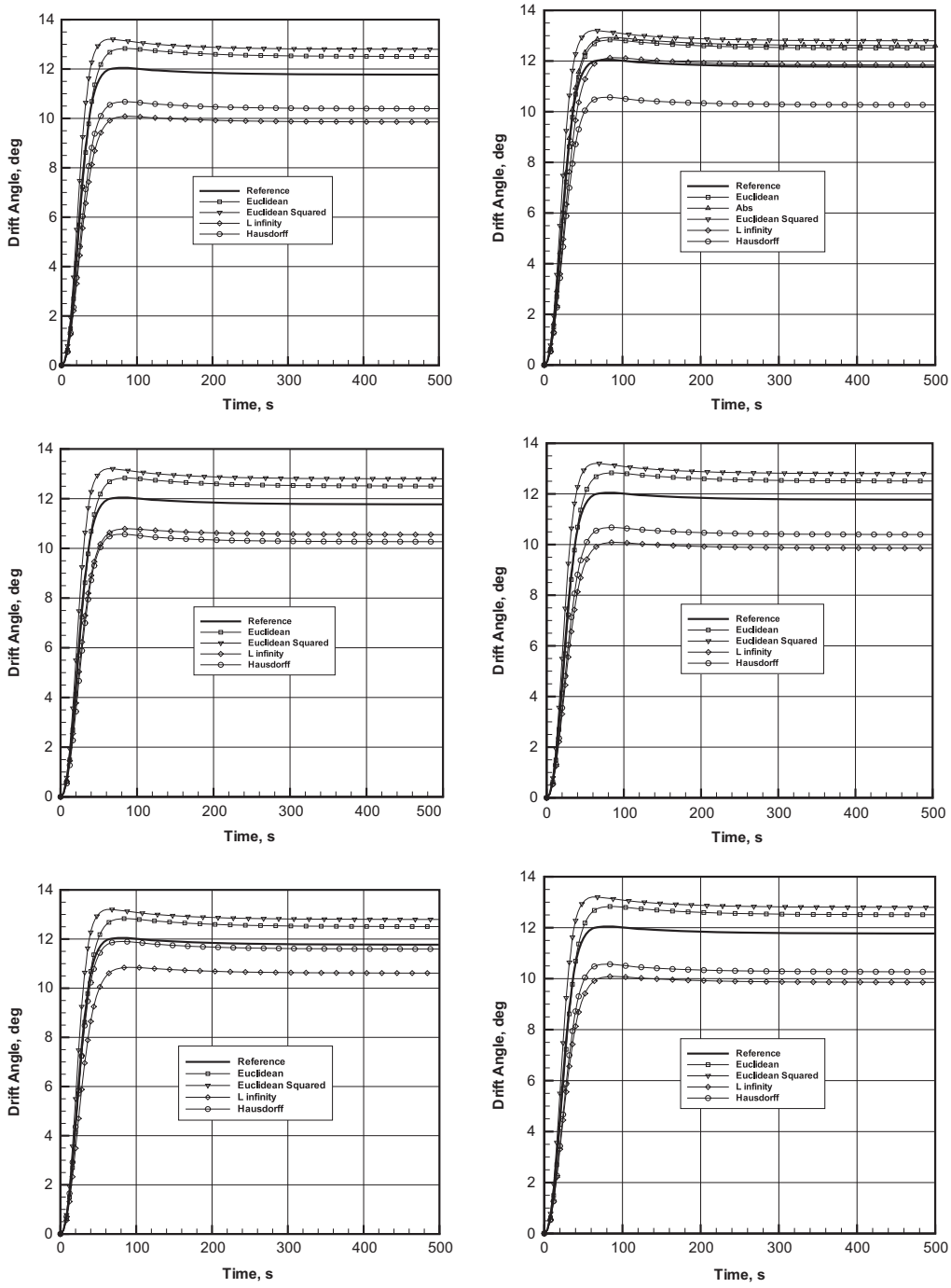

Fig. 11. Time histories $\beta(t)$in the turning manoeuvre for reference and restored models: left—Gauss noise, right—uniform noise; top—noise 5%, middle—noise 20%, bottom—noise 50%.

in Fig. 8. It is clear that the noise introduced in this way corresponds to the so-called "measurement noise" while the real experimental records can be also affected by often unknown external disturbances acting on the ship or scaled model. However, presence of only measurement noise can be considered as sufficient at the first stage.

Estimated adjustment coefficients are given in Table 2 for the case of 50% Gauss noise. Comparison of this table to Table 1 does not show any qualitative differences except that the Euclidean and Absolute Value metrics gave identical results which did not happen in the "clean" case. Inspection of the remaining cases showed similar behaviour of the coefficients (at least with the accuracy of 6–7digits displayed) for other values of the noise level and distribution type. Moreover, these two metrics and the squared Euclidean metric resulted in coefficients independent of the noise except for the 5% Gaussian noise where the results were slightly different. The causes of such excessive robustness have not been completely clarified but the most likely reason is a relatively coarse resolution of chromosomes providing only 256 levels of each coefficient. At the same time, the L-infinity and especially Hausdorff metrics produced much less coincidences of this kind.

The reproduced zigzag responses are presented in Fig. 9 for all tested combinations of metrics and of the noise level and distribution. Analysis of the results revealed the following:

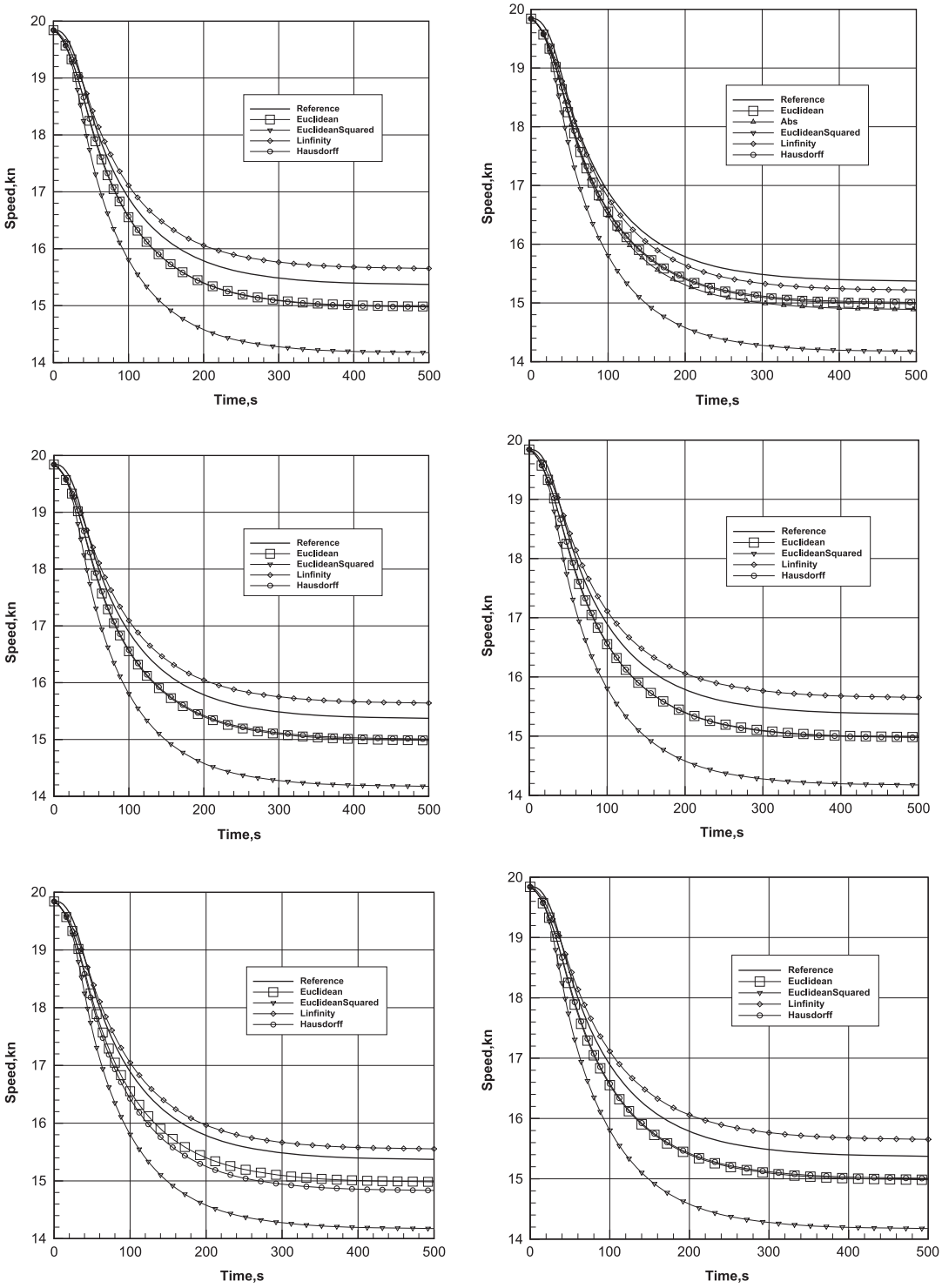

Fig. 12. Time histories $V(t)$in the turning manoeuvre for reference and restored models: left—Gauss noise, right—uniform noise; top—noise 5%, middle—noise 20%, bottom—noise 50%.

1. At first sight, in all the cases the reproducibility of the heading angle response has considerably deteriorated and this is roughly independent of the level and character of the noise. It must be noticed, however, that the most important characteristics i.e. the first and second overshoots in many cases are reproduced approximately correctly. As the zigzag can be interpreted as self-sustained oscillations of a closed-loop dynamic system governed by the nonlinear control law (17), it is possible to talk about the parameters of these oscillations i.e. of their amplitude and period. After the identification, the latter has changed (biased) not very much but enough to result in the progressing divergence of the responses.
2. The L_2- and L_1-metrics gave practically identical results although slight differences in last digits could be traced for some values.
3. The same two metrics and the squared L_2-metric mostly showed the largest discrepancies in the overshoot angles.

Results of validation on the 35° turning manoeuvre are shown in Figs. 10 (time histories for the dimensionless rate of yaw), 11

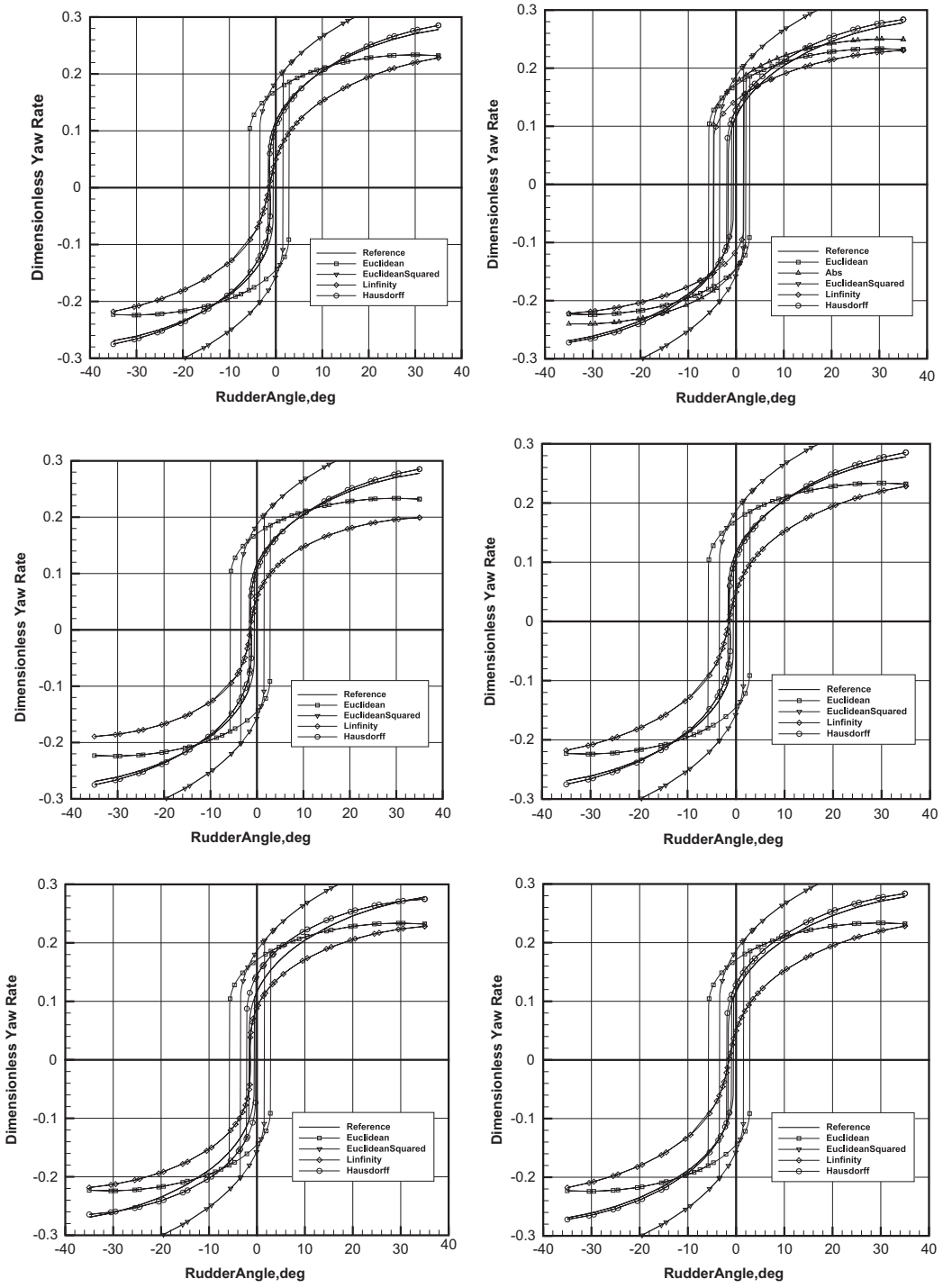

Fig. 13. Spiral curves $r'(\delta_R)$ for reference and restored models: left—Gauss noise, right—uniform noise; top—noise 5%, middle—noise 20%, bottom—noise 50%.

(drift angle). and 12 (speed drop). Regarding the dimensionless rate of yaw transients it can be definitely concluded that the "irregular" squared Euclidean pseudo-metric leads to substantially overestimated peak and asymptotic steady values while the L_∞-metric tangibly underestimates them. The Hausdorff metrics gave the best results just slightly underestimating the peak value. This clear superiority of the Hausdorff metric is, however, lost in reproduction of the drift angle responses: here a more sensitive underestimation (about 1.5°) occurs except, paradoxically, for a rather difficult case of the 50% Gauss noise where this metric worked perfectly. In general, however, the L_2 and L_1 metrics look the best with the overestimation not exceeding one degree in all the cases while the L_∞ metric behaved the worst. But the same metric looked the best in the speed drop time histories (see Fig. 12). The Hausdorff metric worked here just a bit worse and practically identically with the L_2 and L_1 metrics while the squared Euclidean pseudo-metric confirmed its inferiority.

The spiral curves (Fig. 13) showed somewhat unexpected results: practically all metrics with the only exception of the Hausdorff metric have failed resulting in the spiral curves very different from the reference one. The Hausdorff metric, on the contrary, made possible a very reliable recover of this kind of response with slightly worse accuracy in the case of 50% Gaussian noise. It is important that the dimensions of the hysteresis loop

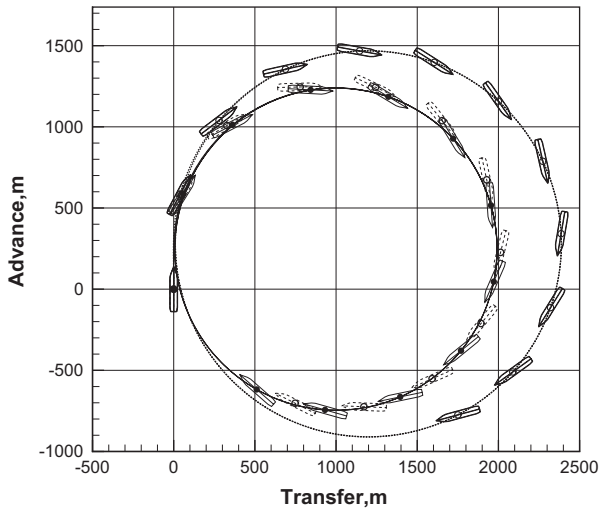

Fig. 14. Turning manoeuvre trajectories (identified from records with 50% Gauss noise): solid line—reference model; dashed line—Hausdorff metric; dotted line—Euclidean metric.

were also reproduced which means correct reproduction of the moderate directional instability characterizing the reference manoeuvring model. The remaining metrics either heavily overestimated the degree of instability, or—in the case of L_∞ metric—lead to a directionally stable model with much lower turning ability.

Finally, trajectories in the 35 turning manoeuvre are shown in Fig. 14 for the Hausdorff and Euclidean metrics demonstrating again clear superiority of the former.

In general, it can be concluded that the developed algorithm is promising as it is capable to perform reasonably accurate and reliable identification of rather complicated ship manoeuvring mathematical models if and only if the Hausdorff metric is used as measure of proximity of the polluted reference responses to the simulated ones. This result was somewhat unexpected: although the Hausdorff metric seems to be a rather natural measure of the distance between sets of values of two functions and it found wide applications in computer vision, the authors were not familiar with attempts to apply it to system identification problems and its definition offers no indications to its discovered surprising robustness.

Of course, as is clear from Eq. (24), this metric is the heaviest from the computational viewpoint but this is not so important for an offline algorithm.

5. Conclusion

A new offline algorithm for identification of ship manoeuvring mathematical models has been developed, tested and validated on a moderately complex manoeuvring model with 19 adjustable parameters. The algorithm was based on the classic genetic algorithm and the objective function was constructed using 5 different metrics including the Hausdorff metric whose application represented a novelty for ship manoeuvring identification problems. Verification and validation were carried out using four simulated time histories resulting from a standard zigzag manoeuvre. These responses were artificially polluted with Gaussian or non-Gaussian white noise with variable level. Non-trivial character of validation was achieved through additional comparisons for the turning and spiral manoeuvres not used for the identification.

The following main conclusions can be drawn from the results of the study:

1. The developed algorithm and code do work correctly: their verification with the clean training responses demonstrated good restoration of the model practically independently of the metric used.
2. The situation changes dramatically when the training processes are polluted with white noise: only the Hausdorff metric proved to be sufficiently robust to provide reasonably good results from noisy records even at substantial noise level.
3. While a dramatic difference in the performance of the algorithm was found when moving from “clean” to even slightly polluted training responses, neither the noise level, nor its distribution did substantially change the identification results.

Although the results obtained so far look quite encouraging, final judgement about the practical value of the developed algorithm can only be obtained after validation on real experimental data. While the measurement noise level will likely be even smaller than applied artificially in this study, there will be environmental disturbances (waves, wind) acting on the ship or its scaled model. While with the model tests it is sometimes possible to minimize the exogenous factors, it is rarely reachable in full-scale trials. Further, the “true” mathematical model will never be identical to the assumed one thus complicating the task even further. All this may implicate certain modifications of the algorithm through introduction of constraints imposed on parameters of the mathematical model whose structure may also be altered.

Acknowledgement

The study was financed by Fundação para a Ciência e a Tecnologia (FCT), Portugal: PTDC/TRA/74332/2006 “Methodology for ship manoeuvring tests using self-propelled models”,

References

Abkowitz, M.A., 1980. Measurements of hydrodynamic characteristics from ship maneuvering trials by system identification. Trans. SNAME 88, 283–318.
Abkowitz, M.A., 1988. Measurements of ship resistance, powering and maneuvering coefficients from simple trials during a regular voyage. Trans. SNAME 96, 97–128.
Araki, M., Sadat-Hosseini, H., Sanada, Y., Tanimoto, K., Umeda, N., Stern, F., 2012. Estimating maneuvering coefficients using system identification methods with experimental, system-based, and CFD free-running trila data. Ocean Eng. 51, 63–84.
Artyszuk, J., 2007. Full scale identification method of four-quadrant hull hydrodynamic coefficients in ship manoeuvring. Arch. Civ. Mech. Eng. VII (3), 20–30.
Åström, K.J., Källström, C.G., 1976. Identification of ship steering dynamics. Automatica 12, 9–22.
Brinati, H.L., A., Rios Neto 1975. Application of the extended Kalman filtering to the identification of ship hydrodynamic coefficients (in Portuguese). In: Proceedings of the Third Brazilian Congress of Mechanical Engineering, vol. C, Rio de Janeiro, pp. 791–804.
Casado, M.H., Ferreiro, R., Velasco, F.J., 2007. Identification of nonlinear ship model parameters based on the turning circle test. J. Ship Res. 51 (2), 174–181.
Crane, C.L., Eda, H., Landsburg, A.C., 1989. Controllability. In: Lewis, E.V. (Ed.), Principles of Naval Architecture, 3. SNAME, Jersey City, NJ, pp. 191–422.
Di Mascio, A., Dubbioso, G., Notaro, C., Viviani, M., 2011. Investigation of twin-screw naval ships maneuverability behavior. J. Ship Res. 55 (4), 221–248.
Faller, W., Hess, D., Smith, W., Huang, T., 1998. Application of Recursive Neural Network Technologies to Hydrodynamics, Twenty-Second Symposium on Naval Hydrodynamics. August 9–14, 1999, National Academy Press, Washington, D.C., pp. 708–723.
Garnier, H., Wang, L. (Eds.), 2008. Springer-Verlag, London
Hensen, H., 1999. Ship Bridge Simulators: a Project Handbook. The Nautical Institute, London
Inoue, S., Hirano, M., Kijima, K., Takashina, J., 1981. A practical calculation method of ship maneuvering motion. Int. Shipbuild. Prog. 28 (325), 207–222.
Källström, C.G., Åström, K.J., 1981. Experiences of system identification applied to ship steering. Automatica 17 (1), 187–198.
Landau, I.,D., Zito, G., 2006. Digital Control Systems. Springer-Verlag, London
Ljung, L., 1987. System Identification: Theory for the User. Englewood Cliffs, New Jersey, Prentice-Hall, Inc.
Ljung, L., Söderström, T., 1983. Theory and Practice of Recursive Identification. The MIT Press, Cambridge, Massachusets, London, England p. 1983
Luo, W.L., Zou, Z.J., 2009. Parametric identification of ship manoeuvring models by using support vector machines. J. Ship Res. 53 (1), 19–30.

Moreira, L., Guedes Soares, C., 2003. Dynamic model of manoeuvrability using recursive neural networks. Ocean Eng. 30 (7), 1669–1697.
Moreira, L., Guedes Soares, C., 2011. Autonomous ship model to perform manoeuvring tests. J. Marit. Res. VIII (2), 29–46.
Moreira, L., Guedes Soares, C., 2012. Recursive neural network model of catamaran manoeuvring. Int. J. Marit. Eng. 154 (Part A3), 121–130.
Nomoto, K., Taguchi, T., Honda, K., Hirano, S., 1957. On the steering qualities of ships. Int. Shipbuild. Prog. 4 (35), 354–370.
Obreja, D., Nabergoj, R., Crudu, L., Păcuraru-Popoiu, S., 2010. Identification of hydrodynamic coefficients for manoeuvring simulation model of a fishing vessel. Ocean Eng. 37, 678–687.
Oltmann, P., S.D. Sharma, 1985. Simulation of combined engine and rudder maneuvers using an improved model of hull-propeller-rudder interactions. In: Proceedings of 15th ONR Symposium on Naval Hydrodynamics. September 2–7, 1984, Hamburg, Washington, D.C., pp. 83–108.
Perera, L.P., Moreira, L., Santos, F.P., Ferrari, V., Sutulo, S., Guedes Soares, C., 2012. A Navigation and Control Platform for Real-Time Manoeuvring Tests of Autonomous Ship Models. In: Proceedings of the 9th IFAC Conference on Manoeuvring and Control of Marine Craft (MCMC 2012). 19–21 September 2012, Arenzano, Italy, Paper no. 87, 6 p.
Rajesh, G., Bhattacharyya, S.K., 2008. System identification for nonlinear maneuvering of large tankers using artificial neural network. Appl. Ocean Res. 30, 256–263.
Rajesh, G., Giri Rajasekhar, G., Bhattacharyya, S.K., 2010. System identification for nonlinear maneuvering of ships using neural network. J. Ship Res. 54 (1), 1–14.
Revestido Herrero, E.R., Velasco González, F.J., 2012. Two-step identification of nonlinear manoeuvring models of marine vessels. Ocean Eng. 53, 72–82.
Rhee, K.-P., Kim, K., 1999. A new sea trial method for estimating hydrodynamic derivatives. J. Ship Ocean Technol. 3 (3), 25–44.
Rockafeller, R.T., Wets, R.J.-B., 2004. Varational Analysis. Springer-Verlag, Berlin, Heidelberg
Silman, G.I., 1988. Creation of mathematical models for ship manoeuvring motion on the basis of full-scale trials′ data (in Russian). In: Gofman, A.D. (Ed.), Propulsion-and-Steering Arrays and Ship Manoeuvring. Sudostroyenie, Leningrad, pp. 82–97
Skjetne, R., Smogeli, Ø.N., Fossen, T.I., 2004. A nonlinear ship manoeuvring model: identification and adaptive control with experiments for a model ship. Modeling, Identif. Control 25 (1), 3–27.
Stern, F., Agdrup, K., Kim, S.Y., Hochbaum, A.C., Rhee, K.P., Quadvlieg, F., Perdon, P., Hino, T., Broglia, R., Gorski, J., 2011. Experience from SIMMAN 2008—the first workshop on verification and validation of ship maneuvering simulation methods. J. Ship Res. 55 (2), 135–147.
Sutulo, S., Guedes Soares, C., 2004. Synthesis of experimental designs of maneuvering captive-model tests with a large number of factors. J. Mar. Sci. Technol. 9, 32–42.
Sutulo, S., Guedes Soares, C., 2005a. Numerical study of some properties of generic mathematical models of directionally unstable ships. Ocean Eng. 32, 485–497.
Sutulo, S., Guedes Soares, C., 2005b. An object-oriented manoeuvring simulation code for surface displacement ships. In: Guedes Soares, C., Garbatov, Y., Fonseca, N. (Eds.), Maritime Transportation and Exploitation of Ocean and Coastal Resources. Taylor & Francis Group, London, pp. 287–294
Sutulo, S., Guedes Soares, C., 2011. Mathematical Models for Simulation of Manoeuvring Performance of Ships. In: Guedes Soares, C., et al. (Eds.), Marine Technology and Engineering. Taylor & Francis Group, London, pp. 661–698In: Guedes Soares, C., et al. (Eds.), Marine Technology and Engineering. Taylor & Francis Group, London, pp. 661–698
Sutulo, S, Guedes Soares, C., 2014. Development of a core mathematical model for arbitrary maneuvers of a shuttle tanker. Appl. Ocean Res. (Accepted for Publication).
Van Maanen, J.D., Van Oossanen, P., 1988. Resistance. In: Lewis, E.V. (Ed.), Principles of Naval Architecture, 2. SNAME, Jersey City, NJ, pp. 1–126.
Viallon, M., Sutulo, S., Guedes Soares, C., 2012. On the order of polynomial regression models for manoeuvring forces, IFAC Conference "Manoeuvring and Control of Marine Craft". 19–21 September 2012, Arenzano, Italy, Paper no. 64, 6 p.
Yoon, H.K., Rhee, K.P., 2003. Identification of hydrodynamic coefficients in ship maneuvering equations of motion by estimation-before-modeling technique. Ocean Eng. 30, 2379–2404.
Zhang, X.-G., Zou, Z.-J, 2011. Identification of Abkowitz model for ship manoeuvring motion using ε-support vector regression. J. Hydrodyn. 23 (3), 353–360.
Zhou, W.W., M. Blanke, 1987. Nonlinear recursive prediction error method applied to identification of ship steering dynamics. In Eighth Ship Control Systems Symposium. October 6–9, vol. 3, The Hague, The Netherlands, pp. 3.85–3.106.